Modeling the Influence of Wall Roughness on Tunnel Propagation

Chenming Zhou and Joseph Waynert

Office of Mine Safety and Health Research
National Institute for Occupational Safety and Health
Pittsburgh, PA 15236, USA
czhou@cdc.gov, jwaynert@cdc.gov

***Abstract*— At the ultra-high frequencies (UHF) common to portable radios, a mine tunnel is often modeled as a hollow dielectric waveguide. The roughness condition of the tunnel walls has an influence on radio propagation and therefore should be taken into account when accurate power predictions are required. In this paper, we derive a general analytical formula for modeling the influence of the wall roughness. The formula can model practical tunnels formed by four dielectric walls, with each having an independent roughness condition. It is found that different modes are attenuated by the same wall roughness in a different way, with higher order modes being significantly more attenuated compared to the dominant mode. The derivation and findings are verified by numerical results based on both ray tracing and modal methods.**

I. Introduction

Radio propagation in tunnels has been investigated for several decades [1]–[4], partially driven by the need for communication among underground miners. Although many methods have been developed, the ray tracing and modal methods are the two major approaches for modeling radio propagation in a straight tunnel.

Unlike road/subway tunnels, underground mine tunnels often have very rough walls which influence the radio signal propagation in the tunnel. Despite the long history of tunnel propagation research, very few investigations have analyzed the influence of roughness on tunnel propagation. One of the earlier models for analyzing the roughness effect was developed by Emslie, who derived an additional mode attenuation constant that accounts for the energy losses caused by the wall roughness to the dominant mode, under the assumption of equal roughness for all four tunnel walls [1].

Considering the fact that the roughness conditions for the four walls of a typical mine entry could be significantly different, we derived a more general analytical roughness model that allows an independent roughness condition for each tunnel wall. The new model is also general to both the dominant mode and higher order modes. We verify the derivation by showing that the simulation results based on the newly developed modal model match the ray tracing based results.

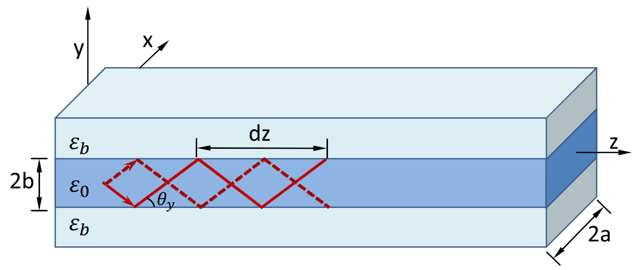

Fig. 1. Geometry of the rectangular dielectric waveguide

II. Modeling the Influence of Wall Roughness

Consider a straight hollow waveguide with rectangular cross-sectional dimensions (2b and 2a as depicted in Fig. 1). Let ϵ_0 denote the permittivity of air, and $\epsilon_{a,b}$ the complex permittivity of the vertical and horizontal walls surrounding the waveguide, respectively. The coordinate system is oriented in the center of the waveguide cross section, with x horizontal, y vertical, and z down the waveguide. The permeability of all media is assumed to be the same and equal to that of the free space μ_0. A transmitter is located at $T(x_0, y_0, 0)$ and a receiver at $R(x, y, z)$. Without loss of generality, we also assume the source is vertically polarized.

A. Modal Method

1) Tunnels with smooth walls: The electric field within a hollow dielectric waveguide with four smooth walls can either be represented by a ray summation based on the ray tracing method or a summation of different modes based on the modal method. For the modal method, the electric field is written as [5], [6]:

$$E_r = \frac{-j2\pi E_t}{ab} \sum_{p=1}^{+\infty} \sum_{q=1}^{+\infty} A_{p,q} \frac{e^{-(\alpha_{p,q}+j\beta_{p,q})z}}{\beta_{p,q}} \tag{1}$$

where E_t is the transmitted electric field, and

$$\begin{aligned} A_{p,q} \;=\; & \sin\left(\tfrac{p\pi}{2a}x+\varphi_p\right)\sin\left(\tfrac{q\pi}{2b}y+\varphi_q\right) \\ & \sin\left(\tfrac{p\pi}{2a}x_0+\varphi_p\right)\sin\left(\tfrac{q\pi}{2b}y_0+\varphi_q\right) \end{aligned} \tag{2}$$

is the mode eigenfunction which reflects the influence of both the transmitter and receiver antenna positions on the power distribution. In addition,

$$\beta_{p,q} = \sqrt{k^2 - \left(\frac{p\pi}{2a}\right)^2 - \left(\frac{q\pi}{2b}\right)^2} \tag{3}$$

$$\alpha_{p,q} = \frac{1}{b}\left(\frac{q\lambda}{4b}\right)^2 \mathrm{Re}\left\{\frac{\bar{\varepsilon}_b}{\sqrt{\bar{\varepsilon}_b - 1}}\right\} + \frac{1}{a}\left(\frac{p\lambda}{4a}\right)^2 \mathrm{Re}\left\{\frac{1}{\sqrt{\bar{\varepsilon}_a - 1}}\right\} \tag{4}$$

are the propagation and attenuation constants, respectively. Here, k is the free space wave vector and $\mathrm{Re}\{\cdot\}$ denotes the real part of the argument. The two phase constants $\varphi_{p,q}$ are defined as:

$$\varphi_{p,q} = \begin{cases} 0 & \text{p(q) is even} \\ \pi/2 & \text{p(q) is odd} \end{cases} \tag{5}$$

As shown in [1], [7], the hybrid mode $EH_{p,q}$ can be viewed as an average of four plane waves (rays), each characterized by the following angles:

$$\theta_y \approx \frac{q\lambda}{4b} \qquad \theta_x \approx \frac{p\lambda}{4a} \tag{6}$$

Note that the approximations in (6) are valid only if the wavelength of interest is small in comparison to the tunnel's transverse dimensions.

Between the two successive reflections on the roof/floor, the ray travels an axial distance of dz (as shown in Fig. 1), which can be calculated as:

$$dz = \frac{2b\cos(\theta_x)}{\tan(\theta_y)} \approx \frac{16b^2}{q\lambda} \tag{7}$$

The number of reflections on the roof/floor that the four rays undergo before they reach the receivers can be computed by

$$N_y = \frac{z}{dz} \approx \frac{q\lambda z}{16b^2} \tag{8}$$

Similarly, the number of reflections on the two side walls is

$$N_x \approx \frac{p\lambda z}{16a^2} \tag{9}$$

The attenuation of the E field caused by all the reflections can be expressed as

$$E_L = \left|\rho_{/\!/}^{2N_y} \cdot \rho_{\perp}^{2N_x}\right| \tag{10}$$

where $|\cdot|$ denotes the magnitude of the argument, and the two reflection coefficients corresponding to the perpendicular and parallel polarizations for smooth walls can be expressed as:

$$\rho_{\perp,/\!/} = \frac{cos\theta_{\perp,/\!/} - \Delta_{\perp,/\!/}}{cos\theta_{\perp,/\!/} + \Delta_{\perp,/\!/}} \tag{11}$$

where

$$\begin{aligned} \Delta_{/\!/} &= \tfrac{\sqrt{\bar{\varepsilon}_b - \sin^2\theta_{/\!/}}}{\bar{\varepsilon}_b} \\ \Delta_{\perp} &= \sqrt{\bar{\varepsilon}_a - \sin^2\theta_{\perp}} \end{aligned} \tag{12}$$

$$\theta_{\perp,/\!/} = \frac{\pi}{2} - \theta_{x,y} \tag{13}$$

Here, $\bar{\varepsilon}_{a,b} = \varepsilon_{a,b}/\varepsilon_0$ are the relative dielectric constants for the vertical and horizontal walls, respectively. For grazing incidences, we can make the following approximations:

$$\rho_{\perp,/\!/} \approx -\exp\left(\frac{-2\cos\theta_{\perp,/\!/}}{\Delta_{\perp,/\!/}}\right) \tag{14}$$

$$\Delta_{/\!/} \approx \tfrac{\sqrt{\bar{\varepsilon}_b - 1}}{\bar{\varepsilon}_b} \quad \Delta_{\perp} \approx \sqrt{\bar{\varepsilon}_a - 1} \tag{15}$$

2) Tunnels with rough walls: Now we consider the rough wall case. We assume that the distribution of the surface variation is a zero mean Gaussian with a standard deviation of $\sigma_{h,i}$ for the i_{th} wall of the tunnel, with the floor as $i = 1$. Under this assumption, a scattering loss factor $\rho_{s,i}$ can be introduced to compensate for the reduced energy in the specular direction of each diffuse reflection [8]:

$$\rho_{s,i} = \exp\left\{-8\left(\frac{\pi\sigma_{h,i}\cos\theta_{\perp,/\!/}}{\lambda}\right)^2\right\} \tag{16}$$

Under the assumption of rough walls, the energy loss given in (10) becomes

$$E_L = \left|\left[\rho_{/\!/}^{2N_y}\left(\rho_{s,1}\rho_{s,3}\right)^{N_y}\right] \cdot \left[\rho_{\perp}^{2N_x}\left(\rho_{s,2}\rho_{s,4}\right)^{N_x}\right]\right| \tag{17}$$

Substituting (6), (8), (9), and (13)-(16) into (17) and after some mathematical manipulations leads to

$$E_L \approx \exp\left\{-\left(\alpha_{p,q} + \alpha^s_{p,q}\right) z\right\} \tag{18}$$

where $\alpha_{p,q}$ is the classic mode attenuation constant given in (4) for tunnels with smooth walls, and

$$\alpha^s_{p,q} = \frac{\pi^2\lambda}{32}\left[\frac{p^3}{a^4}\left({\sigma_{h,2}}^2 + {\sigma_{h,4}}^2\right) + \frac{q^3}{b^4}\left({\sigma_{h,1}}^2 + {\sigma_{h,3}}^2\right)\right] \tag{19}$$

is the roughness attenuation constant for the $EH_{p,q}$ mode.

3) Discussion: Eq. (19) provides a general model for quickly estimating the power loss caused by wall roughness in tunnels. Note that the value of $\alpha^s_{p,q}$ varies for different modes and rapidly increases (approximately cubically with p and q) for higher order modes. For the dominant mode $EH_{1,1}$, and with the assumption of equal roughness σ_h for all the four walls, (19) reduces to

$$\alpha^s_{p,q} = \frac{\pi^2\lambda\sigma_h^2}{16}\left[\frac{1}{a^4} + \frac{1}{b^4}\right] \tag{20}$$

which is exactly the roughness loss factor derived in [1].

It is shown in (19) that given the same roughness, the roughness loss drops rapidly as the dimensions of the tunnel are increased. If the cross section of the tunnel is not square, the roughness on the walls of the greater dimension has a greater effect on the power attenuation. For example, in a high coal mine, the roughness loss is mainly determined by the roughness condition of the two side walls. Note that switching the roughness conditions of the two walls in the same dimension, e.g, $\sigma_{h,1}$ and $\sigma_{h,3}$, does not change the power attenuation.

B. Ray Tracing Method

1) Tunnels with smooth walls: Based on the ray tracing theory, the electric field at an arbitrary point R(x, y, z) within a rectangular waveguide can be obtained by summing the scalar electric fields of the rays from all the images of the point source as [3]:

$$E_r(x,y,z) = E_t \sum_{m=-\infty}^{+\infty} \sum_{n=-\infty}^{+\infty} \frac{e^{-jkr_{m,n}}}{r_{m,n}} \rho_{\perp}^{|m|} \rho_{/\!/}^{|n|} \quad (21)$$

where

$$\begin{array}{rcl} r_{m,n} & = & \sqrt{(x_m - x)^2 + (y_n - y)^2 + z^2} \\ x_m & = & 2ma + (-1)^m x_0 \\ y_n & = & 2nb + (-1)^n y_0 \end{array} \quad (22)$$

The reflection coefficient $\rho_{/\!/,\perp}$ are defined in (11) and approximated by (14) under the grazing incidence assumption. The corresponding incident angles are given by:

$$\theta_{\perp} = \text{acos}\left(|x_m - x|/r_{m,n}\right) \quad \theta_{/\!/} = \text{acos}\left(|y_n - y|/r_{m,n}\right) \quad (23)$$

2) Tunnels with rough walls: For tunnels with rough walls, the electric field is calculated by:

$$E_r = E_t \sum_{m=-\infty}^{+\infty} \sum_{n=-\infty}^{+\infty} \frac{e^{-jkr_{m,n}}}{r_{m,n}} \left(\rho_{\perp}\sqrt{\rho_{s,2}\rho_{s,4}}\right)^{|m|} \left(\rho_{/\!/}\sqrt{\rho_{s,1}\rho_{s,3}}\right)^{|n|} \quad (24)$$

with the roughness loss factor $\rho_{s,i}$ defined in (16).

III. Results

Fig. 2 shows simulated power distributions along the center line of a tunnel under different wall roughness conditions. The measured power distribution in a concrete tunnel with smooth walls is also plotted for reference. The details of the measurement can be found in [3]. The simulated results based on both the modal (dashed line) and ray tracing (marked with circles) methods are compared and shown to agree with each other well. It is apparent that wall roughness introduces additional attenuation to RF signals as well as "smoothness" to the power distribution curve. The "smoothness" effect is due to the fact that higher order modes are attenuated more by the wall roughness than the dominant mode and therefore the rapid fading caused by the presence of higher order modes is quickly eliminated. The major parameters used in the simulations are summarized in Table I.

IV. Conclusion

In this paper, we present some new analysis on the influence of wall roughness based on both modal and ray tracing methods. We extend Emslie's model to a more general form that accounts for higher order modes and can allow independent roughness conditions for different walls. We also show that different methods (the ray tracing and modal methods) yield the same result.

TABLE I
SUMMARY OF PARAMETERS USED IN THE SIMULATION

Parameter	Value	Parameter	Value
Tunnel width (2a)	1.83 m	Re $\{\bar{\epsilon}_{a,b}\}$	8.9
Tunnel height (2b)	2.35 m	$\sigma_{a,b}$	0.15 S/m
Transmitter height	1.22 m	f	2.45 GHz
Receiver height	1.22 m		

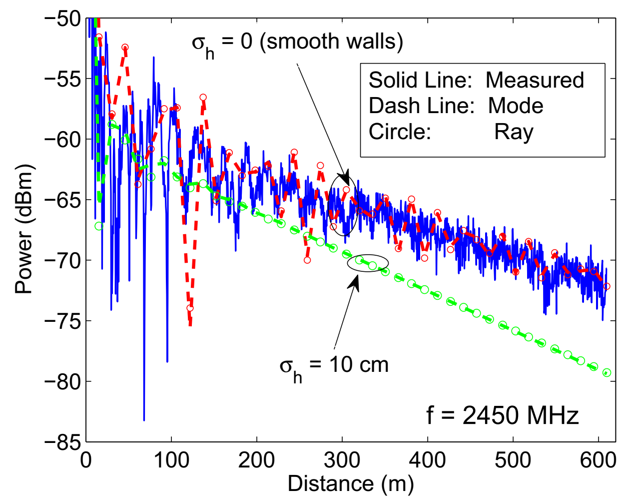

Fig. 2. Power distribution in a hollow dielectric tunnel under different wall roughness conditions.

References

[1] A. Emslie, R. Lagace, and P. Strong, "Theory of the propagation of uhf radio waves in coal mine tunnels," *IEEE Transactions on Antennas and Propagation*, vol. 23, no. 2, pp. 192–205, 1975.

[2] F. Fuschini and G. Falciasecca, "A mixed raysmodes approach to the propagation in real road and railway tunnels," *IEEE Transactions on Antennas and Propagation*, vol. 60, no. 2, pp. 1095–1105, 2012.

[3] C. Zhou, J. Waynert, T. Plass, and R. Jacksha, "Modeling RF propagation in tunnels," in *IEEE International Symposium on Antennas and Propagation (APS2013)*, Orlando, FL, USA, Jul. 2013, pp. 1916–1917.

[4] Z. Sun and I. F. Akyildiz, "Channel modeling and analysis for wireless networks in underground mines and road tunnels," *IEEE Transactions on Communications*, vol. 58, no. 6, pp. 1758–1768, 2010.

[5] K. D. Laakmann and W. H. Steier, "Waveguides: characteristic modes of hollow rectangular dielectric waveguides," *Applied Optics*, vol. 15, no. 5, pp. 1334–1340, 1976.

[6] C. Zhou and J. Waynert, "On the equivalence of the ray tracing and modal methods for modeling radio propagation in tunnels," *To be submitted to IEEE Antennas and Wireless Propagation Letters*, 2013.

[7] C. Zhou, J. Waynert, T. Plass, and R. Jacksha, "Attenuation constants of radio waves in lossy-walled rectangular waveguides," *Progress In Electromagnetics Research*, vol. 142, pp. 75–105, 2013.

[8] W. Ament, "Toward a theory of reflection by a rough surface," *Proceedings of the IRE*, vol. 41, no. 1, pp. 142–146, 1953.

Disclaimer: The findings and conclusions in this paper are those of the authors and do not necessarily represent the views of NIOSH.